Evaluation of a Morphable Anthropomorphic Articulated Total Body Model

Pascoletti, Giulia; Huysmans, Toon; Conti, Paolo; Zanetti, Elisabetta M.

Citation (APA)
Pascoletti, G., Huysmans, T., Conti, P., & Zanetti, E. M. (2022). Evaluation of a Morphable Anthropomorphic Articulated Total Body Model. In C. Rizzi, F. Campana, M. Bici, F. Gherardini, T. Ingrassia, & P. Cicconi (Eds.), *Design Tools and Methods in Industrial Engineering II - Proceedings of the 2nd International Conference on Design Tools and Methods in Industrial Engineering, ADM 2021* (pp. 761-772). (Lecture Notes in Mechanical Engineering). Springer. https://doi.org/10.1007/978-3-030-91234-5_77

Important note
To cite this publication, please use the final published version (if applicable).
Please check the document version above.

Evaluation of a Morphable Anthropomorphic Articulated Total Body Model

Giulia Pascoletti[1,4(✉)] ⓘ, Toon Huysmans[2,3] ⓘ, Paolo Conti[4] ⓘ,
and Elisabetta M. Zanetti[4] ⓘ

[1] Department of Mechanical and Aerospace Engineering (DIMEAS),
Politecnico di Torino, 10129 Turin, Italy
`giulia.pascoletti@polito.it`
[2] Section on Applied Ergonomics and Design, Department of Human Centered Design, Faculty
of Industrial Design Engineering, Delft University of Technology, Delft, The Netherlands
[3] imec-Vision Lab, Department of Physics, University of Antwerp, Antwerp, Belgium
[4] Department of Engineering, University of Perugia, 06125 Perugia, Italy

Abstract. In this work a new approach for the creation of Articulated Total Body
(ATB) models for person-specific multi-body simulations is presented, with the
main aim of overcoming limitations related to classical multi-ellipsoids ATB mod-
els, based on regression equations having only the weight and the height of the
subject as input. The new methodology is based on a Statistical Shape Model
(SSM), morphable according to up to 24 input parameters: the SSM was obtained
from Principal Component Analysis (PCA), applied on a wide database of 3D
human scans (CAESAR). The so obtained geometry can be segmented automat-
ically to generate body segments with the respective inertial properties (mass,
principal moments of inertia, and centres of mass location). The routine has been
tested on a random set of 20 male subjects and the classical multi-ellipsoids models
were compared to these in terms of inertial properties and 3D external geometry:
the highest differences were registered at the abdomen and the thighs for what
concerns the mass (60%), principal moments (75%) and centres of mass (50 mm)
properties; the trunk, the shoulder and the calves are the most critical areas for
the external geometry (average distance between the anthropomorphic and ellip-
soids models equal to 50 mm). A contribution has been made to build person-
specific multibody models. This is a valuable method since approximations made
by multi-ellipsoidal models have resulted to be relevant at specific body areas, and
personalised models can be a support to design and to forensic analyses.

Keywords: Principal component analysis (PCA) · 3D parametric human
model · Articulated total body · Forensic biomechanics · Multibody analysis

1 Introduction

Articulated Total Bodies (ATB) are widely used to simulate human body kinematics in
order to study accidents [1, 2], man-vehicle interactions [3, 4], sport movements [5, 6],
and so on.

These articulated models are usually made of solid bodies, representing human body's segments. Since ATBs are implemented in multibody codes, kinematic (linear and angular displacements, velocities and accelerations) and dynamic (forces and moments) information can be obtained with a limited computational effort [2].

This article is focused on ATB models to be employed for subject-specific analyses (see, for example, forensic biomechanics [7, 8] or subject's specific design [9, 10]). This family of ATBs are usually made of articulated ellipsoids [11, 12]: the geometry and the inertial properties of these ellipsoids are calculated through regression equations, based on surveys information, whose only inputs are the subject's gender, height and weight. As an alternative, anthropomorphic models can be built, where the geometry is obtained through laser scanning [13], CT scans [14], double X-ray exposure [15], photogrammetry [16]; as a next step, the anthropomorphic 3D geometry is segmented in order to identify the above-mentioned body elements and obtain an ATB model. In the latter models, inertial properties (that are the mass, the moments of inertia, the centres of mass) are obtained from segment's geometry, assuming a given density value [12, 17, 18]. In the work here presented, an approach that combines 3D parametric human geometry creation and segmentation is proposed. An anthropomorphic geometry has been created from a limited number of subject measures, morphing a 'standard' geometry; this approach could be implemented thanks to the existence of a wide 3D scans database (CAESAR database [19]), which has been analysed through a Statistical Shape Model (SSM) based on Principal Component Analysis (PCA) [20, 21], in order to establish the key measures to be given as an input to reproduce subject-specific geometry with good details [22, 23].

The performances of the two human modelling approaches are here compared, in order to assess if differences between these two models are significant, and if creating an anthropomorphic model does worth the effort. The anthropomorphic model was here used as reference because it has been proved to be able to replicate the actual human shape with an excellent accuracy (average error equal to 6.59 ± 1.28 mm [22]), while ellipsoidal models are affected by limitations coming from their rough approximation of the actual human shape.

2 Materials and Methods

A set of 20 male adult subjects has been considered, sorting the respective 3D scan from a subset of CAESAR database, referring to Dutch population (518 male human subjects) [19]; these subjects have been chosen randomly trying to cover a wide range of heights (1.62 to 2.05 m), weights (53.6 to 150 kg) and body mass indices BMI, calculated as the weight divided by the square of the height (18 to 40 kg/m^2).

In the following the Statistical Shape Model (SSM) is presented and the new anthropomorphic model is described in detail as well as the respective multi-ellipsoids model.

2.1 Sample Subjects and Statistical Shape Model

The Statistical Shape Model (SSM) implemented for the generation of anthropomorphic 3D geometries is described by the following equation:

$$S_r = \overline{S} + \Phi y \tag{1}$$

where S_r is a new random shape vector (the desired anthropomorphic geometry in this case), $\overline{S}$ is the mean shape based on the overall training data set (S_k) and Φy is the chosen variability model; shape vectors S_r, $\overline{S}$ and S_k are vectors containing 3D human geometry points (nodes). The mean shape is computed based on human 3D scan data: the Generalised Procrustes Analysis was applied in order to align and scale all N shapes in the training set and compute the mean shape as:

$$\overline{S} = \frac{1}{N} \sum_{k=1}^{N} S_k \tag{2}$$

The variability model of the SSM was based on the Principal Component Analysis (PCA), which provides the main modes of variation of the analyzed shapes as eigenvectors: these eigenvectors represent the so-called Principal Components (PCs) and are the column vector of the matrix Φ in Eq. 1. Linear combination of the first PCs (that account for most of the shape variance) are added to the mean shape through the y vector in order to deform the mean shape $\overline{S}$ and generate a new shape vector S_r.

Usually, parameters in the y vector do not have a physical meaning; for this reason, these parameters are linked to physical features representing body characteristics (as height, weight, waist circumference, shoulder breadth, etc.). The relation between these features and the shape model parameters was sought by multiple multivariate linear regression [22]: having defined $\mathbf{f} = [f_1, f_2, \ldots, f_F, 1]^T$ as the feature vector of a specific body shape (that is the vector containing the F selected features), the PC weights y of a body shape with feature f can be generated as:

$$y = Mf \tag{3}$$

where M is the mapping matrix defining the relationship between y and f.

For the subjects' set here considered, 10 measurements have been chosen as input features (Fig. 1); these parameters have been identified, among 24 available, as the measurements playing the highest influence on the actual human shape, according to statistical regressions [22]. The following figure shows the comparison between the average shape (blue shape) and two different body shapes belonging to the subjects' set considered.
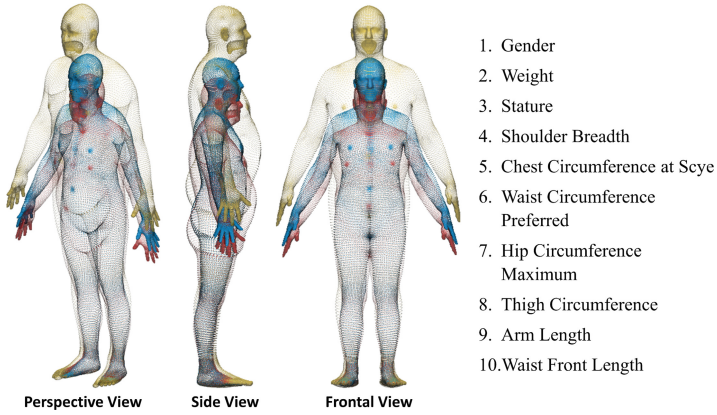
1. Gender
2. Weight
3. Stature
4. Shoulder Breadth
5. Chest Circumference at Scye
6. Waist Circumference Preferred
7. Hip Circumference Maximum
8. Thigh Circumference
9. Arm Length
10. Waist Front Length

Perspective View   **Side View**   **Frontal View**

Fig. 1. Average shape (blue shape) and two different body shapes (yellow and red shapes) belonging to the set of 20 subjects

2.2 Anthropomorphic Model

The external geometry of the anthropomorphic model was obtained with a dedicated software [21] created at the Delft University of Technology and based on the Statistical Shape model described in Sect. 2.1; this code is able to generate the outer subject geometry for a maximum set of 24 anthropometric measurements. The standard model (average shape, Fig. 2b) and the subject-specific model (predicted shape, Fig. 2a and c) share iso-topological meshes and include anatomical landmarks (blue and yellow nodes in Fig. 2) also derived from the CAESAR data.
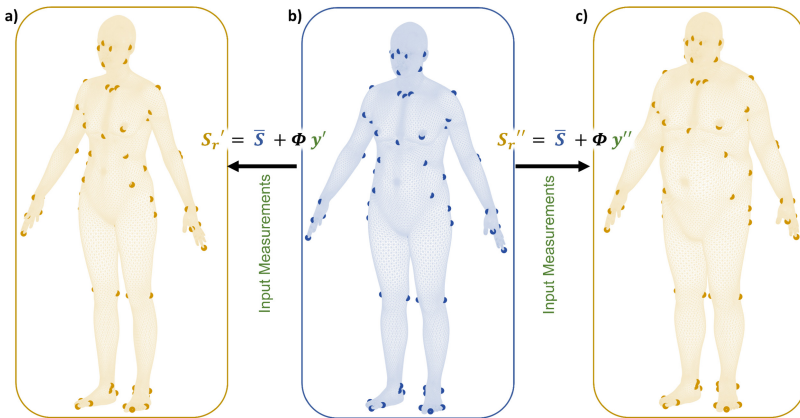

$$S_r' = \bar{S} + \Phi\, y'$$

$$S_r'' = \bar{S} + \Phi\, y''$$

Input Measurements

Fig. 2. a) Predicted shape for a female subject; b) Average shape; c) Predicted shape for a male subject. Blue and yellow nodes represent anatomical landmarks

The anthropomorphic 3D models were segmented into 15 components (Fig. 3b, c): this operation was made on the standard geometry, using anatomical segmenting planes (grey planes in Fig. 3a) built with reference to anatomical landmarks (Fig. 2b).

Mesh nodes belonging to each body segment were defined by a point cloud that represents the set of nodes which lies between two or more planes of segmentation.

These nodes were identified using the sign property of the dot product between two vectors *a* and *b*: *a* is the normal vector of the segmenting plane and *b* is defined as the vector of the distance between a point lying on this plane and nodes of the average shape geometry (Fig. 3a).

All sets of nodes were so obtained on the average shape (Fig. 3b), along with the respective identification numbers; in this way the segmentation can be easily transferred to any predicted shape generated by the code (Fig. 3c) thanks to mesh iso-topology.
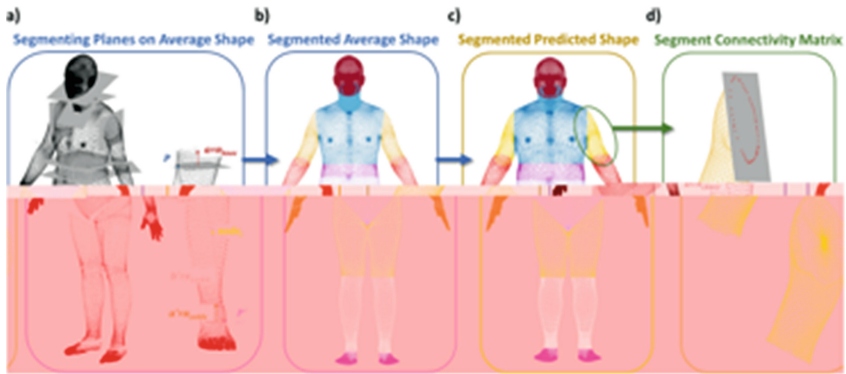

Fig. 3. a) Segmenting planes on the average shape and segments' nodes analytical definition; b) Segmented average shape; c) Segmented predicted shape; d) Segment connectivity matrix

A closed mesh representing a manifold geometry is required in order to create the multibody ATB model. For this reason, additional nodes and triangles have been added to the boundary regions of the segment, with the final aim of closing the open segment's portions (Fig. 3d).

In the next step, the inertial properties of each segment are calculated from the respective geometry, assuming an average constant density ρ, equal to:

$$\rho = \frac{M_{TOT}}{V_{TOT}} \tag{4}$$

where M_{TOT} is the subject weight in kg and V_{TOT} is the respective volume in m^3 calculated on the anthropomorphic geometry.

2.3 Multi-ellipsoid Model

The multi-ellipsoids model is made of 15 ellipsoids, articulated at anatomical joints position (Fig. 4). Given the input weight and height, the subject gender (all males), and its age range (all adults), 32 anthropometric measurements can be derived, according to regression equations obtained by USAF (United States Air Force) on 2420 male

subjects [24]. The geometry (semiaxes length) and the inertial properties (centres of mass, weight, principal moments of inertia) of the 15 ellipsoids are then derived from these anthropometric measurements through regression equations.
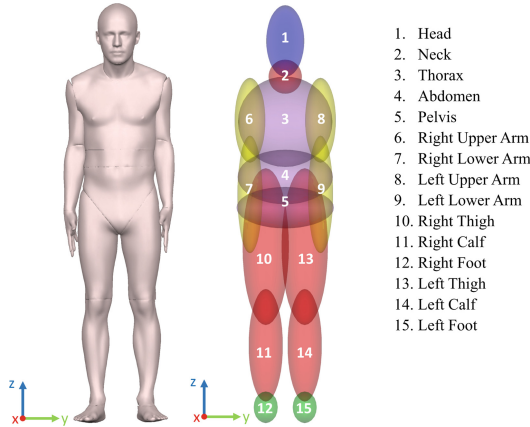

Fig. 4. Anthropomorphic and multi-ellipsoid model

2.4   Comparison Between the Ellipsoids Model and the Anthropomorphic Model

The comparison between the ellipsoids model and the anthropomorphic one, has included the analysis of the following properties:

- Inertial properties: mass, principal moments of inertia, centre of mass location
- 3D geometry

As stated in the Introduction section, the anthropomorphic model was used as reference for these analyses, due to its high and known accuracy in replicating the actual human shape (average error equal to 6.59 ± 1.28 mm [22]).

The reference system reported in Fig. 4 has been used: x is the posterior-anterior axis; y is the medio-lateral axis, directed from the plane of symmetry to the left of the subject; z is the vertical axis, directed upwards.

Inertial Properties. The following entities have been considered:

- Principal moments of inertia ($I_{xx_{i,j,k}}, I_{yy_{i,j,k}}, I_{zz_{i,j,k}}$)
- Masses ($M_{i,j,k}$)
- Centers of mass position ($CM_{x_{i,j,k}}, CM_{y_{i,j,k}}, CM_{z_{i,j,k}}$)

where i is the segment ($i = 1$ to 15), j is the subject being considered ($j = 1$ to 20), k is the model being assessed ('E' for ellipsoids model, 'A' for anthropomorphic model).

Differences between values calculated for the ellipsoids model or for the anthropomorphic one have been analysed both in absolute (e_{abs}) and relative (e_{rel}) terms for all inertial properties; for example, considering I_{xx}:

$$e_{I_{xx},i,j,abs} = I_{xx,i,j,E} - I_{xx,i,j,A} \tag{5}$$

$$e_{I_{xx},i,j,rel} = \frac{\mu I_{xx}, i}{\mu A, I_{xx}, i} \cdot 100 \tag{6}$$

For both e_{abs} and e_{rel}, mean and standard deviation parameters have been considered.

The position of the centers of mass has been analyzed using the abdomen center of mass as a reference; the reason is that the whole body center of mass can be roughly approximated with the abdomen center of mass [25, 26]. Given the subject j, the 3D geometry of the ellipsoids' model was translated in order to make abdominal centers of mass coincide with the abdominal centers of mass of the anthropomorphic model. In the next step, the vertical distance (along z axis) between $CM_{z_{i,j,A}}$ and $CM_{z_{i,j,E}}$ was assessed for all segments. This analysis results in incremental errors moving from the abdomen center of mass to the farthest centers of mass; a second analysis was therefore performed where the reference center of mass changed from segment to segment according to Table 1. The vertical distance has been considered in place of the Euclidean distance because the second one has resulted to be heavily influenced by small difference in posture between the two models.

Paired-samples Wilcoxon tests have been used to assess, segment by segment, if differences between the anthropomorphic and ellipsoidal models were significant.

Table 1. Reference segments for relative centres of mass distance

Segment	Reference segment	Segment	Reference segment
1. Head	2. Neck	8. Left Upper Arm	3. Thorax
2. Neck	3. Thorax	9. Left Forearm	8. Left Upper Arm
3. Thorax	4. Abdomen	10. Right Thigh	5. Pelvis
4. Abdomen	–	11. Right Calf	10. Right Thigh
5. Pelvis	4. Abdomen	12. Right Foot	11. Right Calf
6. Right Upper Arm	3. Thorax	13. Left Thigh	5. Pelvis
7. Right Forearm	6. Right Upper Arm	14. Left Calf	13. Left Thigh

3D Geometry. 3D geometries have been compared considering, node by node, the Euclidean 'nearest neighbor distance'. The average distance d_{ave} has been calculated among all nodes as well as the 90% percentile distance d_{90}.

An F-test was performed in order to test if the variance of distances d_{ave} was significantly greater than the variance of distances measured between the anthropomorphic model and the true body shape, as reported in [22].

3   Results and Discussion

3.1   Inertial Properties

Figure 5 shows results of the absolute error analysis for the inertial parameters.

Ideally the absolute error for all the segments would be close to zero (black line in Fig. 5) if the ellipsoids model was able to provide a perfect estimate.

For most of the segments the approximation related to the ellipsoids model is very good, indeed the absolute error is low and approximately constant for all the subjects.

This approximation is not equally good for all segments: for example, data referring to the abdomen (blue circles) and the pelvis (red circles) are systematically below zero, pointing out that for these segments the relative inertial properties are systematically underestimated; on the contrary, data referring to the thorax (light blue circles) and the thighs (yellow and pink circles) are systematically overestimated. According to this evidence, ellipsoids model provides a very good approximation of inertial properties calculated from the actual geometry.
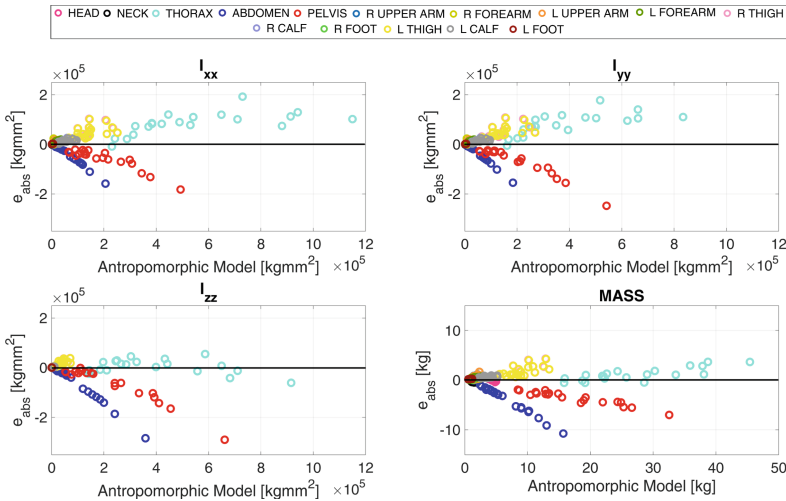

Fig. 5. Absolute error analysis results for inertial parameters: absolute errors are plotted versus the respective anthropomorphic model's inertial data

These findings are confirmed also by the analysis of relative errors (Eq. 6): in particular the abdomen remains critical also with reference to this parameter, whose average value is larger than 65% for the moments of inertia and about 60% for the mass estimation.

As a general rule, the ellipsoids model provides a better approximation of the mass compared to inertial moments.

Distances of centres of mass between the anthropomorphic model and the ellipsoids' one has evidenced major errors (>25 mm) for the upper arms ($\mu \approx 35$ mm), thighs ($\mu \approx 53$ mm), calves ($\mu \approx 54$ mm) and feet ($\mu \approx 100$ mm). However, when the nearest segments are taken as a reference, the head ($\mu \approx 35$ mm), the neck ($\mu \approx 34$ mm) and

the forearms ($\mu \approx 40$ mm) and thighs ($\mu \approx 34$ mm) have resulted to be more critical: these are the key segments which determine errors observed in Fig. 6b.
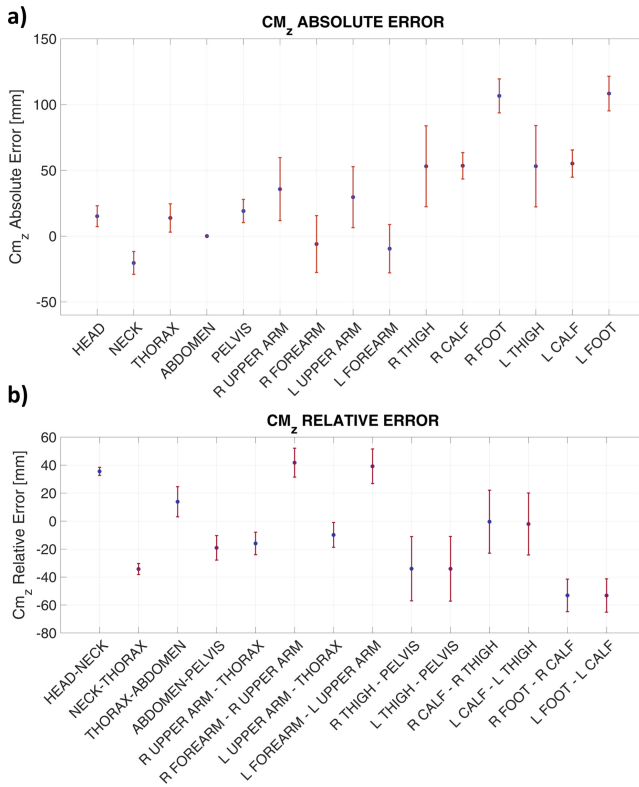

Fig. 6. Analysis of the centres of mass error distribution along the z coordinate with respect the abdomen (a) and with respect the nearest segment (b)

According to Wilcoxon paired tests, inertial parameters are significantly different between the anthropomorphic and the ellipsoids model ($p < 0.01$), exception made for the head mass, thorax moment of inertia I_{zz} and the right forearm CM_z.

3.2 3D Geometry

The distribution of the Euclidean distance between respective nodes has resulted to be consistent among all 20 subjects, with the most critical areas located at shoulders, arms and calves (Fig. 7). A 90th percentile value equal to about 50 mm has been assessed and an average distance of 23 ± 7.39 mm has been computed; errors can get greater for obese subjects, especially in the trunk where they reach values larger than 130 mm.

Figure 7 a, b and c show the geometrical error distribution for a normal-weight, an over-weight and an under-weight subject respectively.
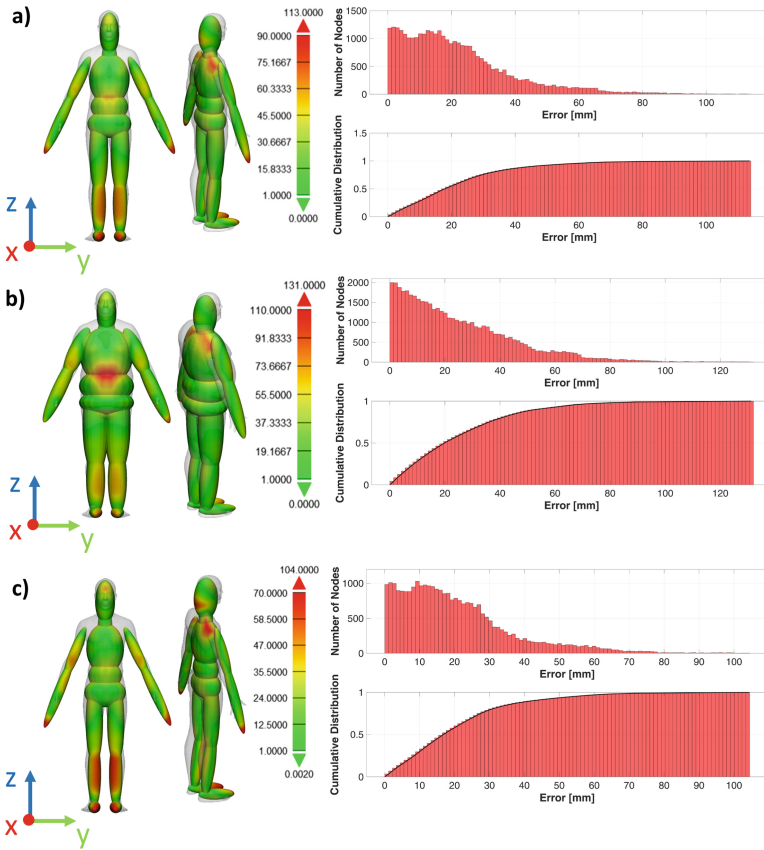
Fig. 7. Geometric distribution error analysis for: a) normal-weight subject; b) over-weight subject; c) under-weight subject

The F-test has shown that the variance of d_{ave} (that is the ellipsoidal geometry deviation from the anthropomorphic one) is significantly greater than the variance of distances measured between the anthropomorphic model and the true body shape. In other words, the ellipsoids model is affected by a significant added source of error, coming from the geometrical approximation through ellipsoids.

4   Conclusions

This work was finalised to assess if creating an ATB model from an anthropomorphic model did worth the effort providing significantly better accuracy in geometrical reconstruction and significantly different values of inertial total bodies. The analysis has given positive results: the statistical relevance of differences between the two analysed models has been proved. With reference to inertial properties, only a limited number of segments (head, thorax and right forearm) has exhibited weak significance of differences, coming from the associated absolute error being very limited. More in detail, with reference to

the ellipsoids model, the abdomen and the thighs are the most critical segments for what concerns inertial properties, while when the external geometry is considered, the most critical areas are located at the shoulders, the calves, and, for obese subjects, at the trunk. The ellipsoids model errors concerning mass estimation can reach 60%, those concerning inertial moments 75%; the centres of mass can result to be displaced up to 50 mm; distances between the actual geometry and ellipsoids geometry can reach 130 mm for most obese patients, while in most cases they remain below 50 mm.

In this work the anthropomorphic ATB model has been used as reference for the performed analyses, due to its ability to more accurately replicate the actual human geometry. In light of this, it was assumed that also inertial properties computed from segments' geometries and density are most reliable than those provided by regression equations. The differences between the two models could have a significant impact on the outcome of multibody analyses, especially when the human subject geometry interacts with the external environment.

On the whole, the methodology here presented wants to give a contribution to the field of human body modelling, with particular reference to the subject-specific models where the novel approach was proved to provide a significantly more accurate method for segments' properties definition.

References

1. Cheng, Z., Rizer, A.L., Pellettiere, J.A.: Modeling and simulation of OOP occupant-airbag interaction. SAE Trans. **112**, 565–575 (2003). https://doi.org/10.4271/2003-01-0510
2. Haug, E., Choi, H.Y., Robin, S., Beaugonin, M.: Computational Models for the Human Body. Elsevier, Ansterdam (2004)
3. Shang, S., et al.: The predictive capacity of the MADYMO ellipsoid pedestrian model for pedestrian ground contact kinematics and injury evaluation. Accid. Anal. Prev. **149**, 105803 (2021). https://doi.org/10.1016/j.aap.2020.105803
4. Crocetta, G., Piantini, S., Pierini, M., Simms, C.: The influence of vehicle front-end design on pedestrian ground impact. Accid. Anal. Prev. **79**, 56–69 (2015). https://doi.org/10.1016/j.aap.2015.03.009
5. Shewchenko, N., Withnall, C., Keown, M., Gittens, R., Dvorak, J.: Heading in football. Part 2: biomechanics of ball heading and head response. Br. J. Sports Med. **39**, i26–i32 (2005). https://doi.org/10.1136/bjsm.2005.019042
6. LifeMOD Tutorials Bicycle Rider. http://www.lifemodeler.com/LM_Manual_2010/T_bike.shtml. Accessed 27 Jan 2021
7. Muggenthaler, H., Drobnik, S., Hubig, M., Schönpflug, M., Mall, G.: Fall from a Balcony-accidental or homicidal? Reconstruction by numerical simulation. J. Forensic Sci. **58**, 1061–1064 (2013). https://doi.org/10.1111/1556-4029.12148
8. Pascoletti, G., Catelani, D., Conti, P., Cianetti, F., Zanetti, E.M.: Multibody models for the analysis of a fall from height: accident, suicide, or murder? Front. Bioeng. Biotechnol. **7**, 419 (2019). https://doi.org/10.3389/fbioe.2019.00419
9. Cessna Aircraft Company: Methodology for seat design and certification by analysis (revision A) (2001)
10. Gavelin, A., Lindquist, M., Oldenburg, M.: Modelling and simulation of seat-integrated safety belts including studies of pelvis and torso responses in frontal crashes. Int. J. Crashworthiness **12**, 367–379 (2007). https://doi.org/10.1080/13588260701482906

11. TNO: MADYMO Human Body Models Manual (2012)
12. Gross, M.E.: THE GEBODIII Program User's Guide and Description (1991)
13. Corazza, S., Mündermann, L., Chaudhari, A.M., Demattio, T., Cobelli, C., Andriacchi, T.P.: A markerless motion capture system to study musculoskeletal biomechanics: visual hull and simulated annealing approach. Ann. Biomed. Eng. **34**, 1019–1029 (2006). https://doi.org/10.1007/s10439-006-9122-8
14. Andersson, B., Valfridsson, M.: Digital 3D facial reconstruction based on computed tomography (2005). www.ep.liu.se/exjobb/itn/2005/mt/010/
15. Hosseinian, S., Arefi, H.: 3D reconstruction from multi-view medical X-ray images - review and evaluation of existing methods. Int. Arch. Photogramm. Remote Sens. Spat. Inf. Sci. ISPRS Arch. **40**, 319–326 (2015). https://doi.org/10.5194/isprsarchives-XL-1-W5-319-2015
16. Remondino, F.: Three-dimensional reconstruction of static human body with a digital camera. In: Proceedings of SPIE - The International Society for Optical Engineering, pp. 38–45. SPIE Digital Library (2003). https://doi.org/10.1117/12.473090
17. Penmatsa, R., et al.: Estimation of mass and inertia properties of human body segments for physics-based human modeling and simulation applications. SAE Int. J. Passeng. Cars - Mech. Syst. **2**, 1626–1631 (2009). https://doi.org/10.4271/2009-01-2301
18. Ma, Y., Lee, K., Li, L., Kwon, J.: Nonlinear regression equations for segmental mass-inertial characteristics of Korean adults estimated using three-dimensional range scan data. Appl. Ergon. **42**, 297–308 (2011). https://doi.org/10.1016/j.apergo.2010.07.005
19. Robinette, K.M., et al.: Civilian American and European Surface Anthropometry Resource (Caesar). Final report, volume I: summary (2002). https://doi.org/10.1093/milmed/137.11.407
20. Pascoletti, G., Calì, M., Bignardi, C., Conti, P., Zanetti, E.M.: Mandible morphing through principal components analysis. In: Rizzi, C., Andrisano, A.O., Leali, F., Gherardini, F., Pini, F., Vergnano, A. (eds.) ADM 2019. LNME, pp. 15–23. Springer, Cham (2020). https://doi.org/10.1007/978-3-030-31154-4_2
21. Huysmans, T., Molenbroek, J.F.M.: DINED Mannequin. Tijdschrift voor Human Factors (45), 4–7 (2020)
22. Danckaers, F., Huysmans, T., Sijbers, J.: Adaptable digital human models from 3D body scans. In: DHM Posturography, pp. 459–470 (2019). https://doi.org/10.1016/B978-0-12-816713-7.00033-7
23. Danckaers, F., Huysmans, T., Lacko, D., Sijber, J.: Evaluation of 3D body shape predictions based on features, pp. 258–265 (2015). https://doi.org/10.15221/15.258
24. Grunhofer, H.J., Kroh, G.: A review of anthropometric data of German Air Force and United States Air Force flying personnel 1967–1968. Appl. Ergon. **7**, 110–111 (1976). https://doi.org/10.1016/0003-6870(76)90172-1
25. Mcconville, J.T., Churchill, T.: Anthropometric Relationships of Body and Body Segment Moments of Inertia. Report, vol. 105, pp. 7405–7409 (1980). https://doi.org/10.1073/pnas.0710346105
26. Young, J.W., Chandler, R.F., Snow, C.C., Robinette, K.M., Zehner, G.F., Lofberg, M.S.: Anthropometric and Mass Distribution Characteristics of the Adult Female (1983)